MATERIALS AND SCIENCE IN SPORTS

Edited by:
F.H. (Sam) Froes and S.J. Haake

Dynamics

Sports Ball Aerodynamics: Effects of Velocity, Spin and Surface Roughness

Rabindra D. Mehta and Jani Macari Pallis

Pgs. 185-197

TMS
184 Thorn Hill Road
Warrendale, PA 15086-7514
(724) 776-9000

SPORTS BALL AERODYNAMICS: EFFECTS OF VELOCITY, SPIN AND SURFACE ROUGHNESS

Rabindra D. Mehta
NASA Ames Research Center,
Moffett Field, California, USA

Jani Macari Pallis
Cislunar Aerospace, Inc., San Francisco, California, USA

Abstract

Aerodynamic principles affect the flight of a sports ball as it travels through the air. From the design of dimples on a golf ball or the curved flight path of a tennis, cricket or baseball, aerodynamics affects speed, motion (position and placement) and ultimately athletic performance.

The aerodynamics of several different sports balls, including baseballs, golf balls, tennis balls, cricket balls, volleyballs and soccer balls are discussed with the help of recent wind tunnel measurements and theoretical analyses. An overview of basic sports ball aerodynamics as well as some new flow visualization data and aerodynamic force measurements are presented and discussed. The materials include explanations of basic fluid dynamics principles, such as Bernoulli's theorem, circulation, the four flow regimes a sphere or a sports ball encounters, and laminar and turbulent boundary layers. The effects of these specific mechanisms on the behavior and performance of sports balls are demonstrated. The specific aerodynamics of the strategic pitches, serves, kicks and strokes used in each sport are described. In particular, the effects of surface roughness and spin on the behavior of the boundary layers and the critical Reynolds number are discussed here.

For spinning balls, the Magnus effect, which is responsible for producing the side or lift force, is discussed in detail, as well as the conditions under which a negative or reverse Magnus effect can be created. It is interesting to note that except for golf and cricket, the ball in all the other games included in the present discussion undergoes a flight regime when the ball is not spinning. The role of the surface roughness, especially if it can be used to generate an asymmetric flow, becomes even more critical for these cases. This paper compares and contrasts the unique aerodynamic characteristics of a variety of sports balls.

The materials presented are a rigorous treatment of the authors' educational sports science work (http://wings.ucdavis.edu/Book/Sports).

Materials and Science in Sports
Edited by F.H. (Sam) Froes
TMS (The Minerals, Metals & Materials Society), 2001

Introduction

Aerodynamics plays a prominent role in defining the flight of a ball that is struck or thrown through the air in almost all ball sports. The main interest is in the fact that the ball can be made to deviate from its initial straight path, resulting in a curved, or sometimes an unpredictable, flight path. Lateral deflection in flight, commonly known as swing, swerve or curve, is well recognized in baseball, cricket, golf, tennis, volleyball and soccer. In most of these sports, the lateral deflection is produced by spinning the ball about an axis perpendicular to the line of flight. In the late 19^{th} century, Lord Rayleigh credited the German scientist, Gustav Magnus, with the first true explanation of this effect and it has since been universally known as the *Magnus effect.* This was all before the introduction of the boundary layer concept by Ludwig Prandtl in 1904. It was soon recognized that the aerodynamics of sports balls was strongly dependent on the detailed development and behavior of the boundary layer on the ball's surface.

A side force, which makes a ball swing through the air, can also be generated in the absence of the Magnus effect. In one of the cricket deliveries, the ball is released with the seam angled, which creates the boundary layer asymmetry necessary to produce swing. In baseball, volleyball and soccer there is an interesting variation whereby the ball is released without any spin imparted to it. In this case, depending on the seam or stitch orientation, an asymmetric, and sometimes time-varying, flow field can be generated, thus resulting in an unpredictable flight path. Almost all ball games are played in the Reynolds Number range of between about 40,000 to 400,000. The Reynolds number is defined as, $Re = Ud/\nu$, where U is the ball velocity, d is the ball diameter and ν is the air kinematic viscosity. It is particularly fascinating that, purely through historical accidents, small disturbances on the ball surface, such as the stitching on baseballs and cricket balls, the felt cover on tennis balls and patch-seams on volleyballs and soccer balls, are about the right size to affect boundary layer transition and development in this Re range.

There has been a lot of research on sportsball aerodynamics since the last review article on the topic was published by Mehta in 1985 (1). Some new data on the three balls (cricket ball, baseball and golf ball), which were covered in that review article are presented. In addition, the aerodynamics of tennis balls, volleyballs and soccer balls are also discussed here. The flow regimes are presented and discussed using recent flow visualization data and wind tunnel measurements of the aerodynamic forces that are generated on the balls.

Basic Aerodynamic Principles

Let us first consider the flight of a smooth sphere through an ideal or inviscid fluid. As the flow accelerates around the front of the sphere, the surface pressure decreases (*Bernoulli equation*) until a maximum velocity and minimum pressure are achieved half way around the sphere. The reverse occurs over the back part of the sphere so that the velocity decreases and the pressure increases (adverse pressure gradient). In a real viscous fluid such as air, a boundary layer, defined as a thin region of air near the surface, which the sphere carries with it is formed around the sphere. The boundary layer cannot typically negotiate the adverse pressure gradient over the back part of the sphere and it will tend to peel away or "separate" from the surface. The pressure becomes constant once the boundary layer has separated and the pressure difference between the front and back of the sphere results in a drag force that slows down the sphere. The boundary layer can have two distinct states: "laminar", with smooth tiers of air passing one on top of the other, or "turbulent", with the air moving chaotically throughout the layer. The turbulent boundary layer has higher momentum near the wall, compared to the laminar layer, and it is continually replenished by turbulent mixing and transport. It is therefore better able to withstand the adverse pressure gradient over the back part of the sphere and, as a result, separates relatively late compared to a laminar boundary layer. This results in a smaller separated region or "wake"

behind the ball and thus less drag. The "transition" from a laminar to a turbulent boundary layer occurs when a critical sphere Reynolds number is achieved.

The flow over a sphere can be divided into four distinct regimes (2). These regimes are illustrated in Fig. 1, in which the drag coefficient (C_D) is plotted against the Reynolds number (Re). The drag coefficient is defined as, $C_D = D/(0.5\rho U^2 A)$, where D is the drag force, ρ is the air density and A is the cross-sectional area of the sphere. In the subcritical regime, laminar boundary layer separation occurs at an angle from the front stagnation point (θ_s) of about 80° and the C_D is nearly independent of Re. In the critical regime, the C_D drops rapidly and reaches a minimum at the critical Re. The initial drop in C_D is due to the laminar boundary layer separation location moving downstream ($\theta_s \cong 95°$). At the critical Re, a separation bubble is established at this location whereby the laminar boundary layer separates, transition occurs in the free-shear layer and the layer reattaches to the sphere surface in a turbulent state. The turbulent boundary layer is better able to withstand the adverse pressure gradient over the back part of the ball and separation is delayed to $\theta_s \cong 120°$. In the supercritical regime, transition occurs in the attached boundary layer and the C_D increases gradually as the transition and the separation locations creep upstream with increasing Re. A limit is reached in the transcritical regime when the transition location moves all the way upstream, very close to the front stagnation point. The turbulent boundary layer development and separation is then determined solely by the sphere surface roughness, and the C_D becomes independent of Re since the transition location cannot be further affected by increasing Re.

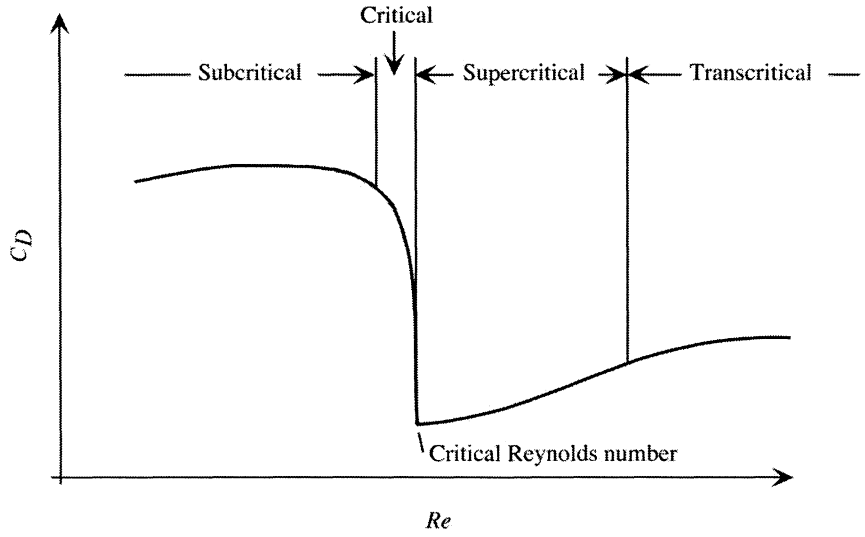

Figure 1: Flow regimes on a sphere.

Earlier transition of the boundary layer can be induced by "tripping" the laminar boundary layer using a protuberance (e.g. seam on a baseball or cricket ball) or surface roughness (e.g. dimples on a golf ball or fabric cover on a tennis ball). The C_D versus Re plot shown in Fig. 2 contains data for a variety of sports balls together with Achenbach's (2) curve for a smooth sphere. All these data are for non-spinning test articles, and all except the cricket ball, were held stationary in wind tunnels for the drag measurements. The cricket ball was projected through a wind tunnel test section and the drag determined from the measured deflection. For the smooth sphere, the C_D in the subcritical regime is about 0.5 and at the critical Re of about 400,000 the C_D drops to a minimum of about 0.07, before increasing again in the supercritical regime. The critical Re, and amount by which the C_D drops, both decrease as the surface roughness increases on the sports balls. The specific trends for each of the sports balls are discussed below in the individual ball sections.

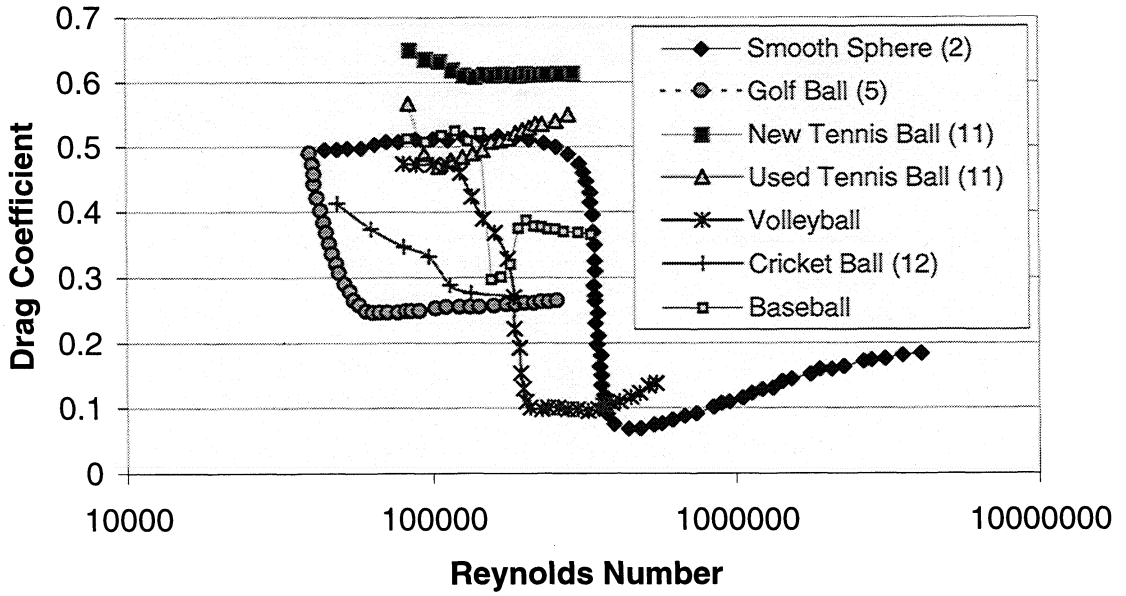

Figure 2: Drag coefficient versus Reynolds number for different sports balls. Volleyball data courtesy of Don Geister, Aerospace Department, University of Michigan.

In a viscous flow such as air, a sphere that is spinning at a relatively high rate can generate a flow field that is very similar to that of a sphere in an inviscid flow with added circulation. That is because the boundary layer is forced to spin with the ball due to viscous friction, which produces a circulation around the ball, and hence a side force. At more nominal spin rates, such as those encountered on sports balls, the boundary layers cannot negotiate the adverse pressure gradient on the back part of the ball and they tend to separate, somewhere in the vicinity of the sphere apex. The extra momentum applied to the boundary layer on the retreating side of the ball allows it to negotiate a higher pressure rise before separating and so the separation point moves downstream. The reverse occurs on the advancing side and so the separation point moves upstream, thus generating an asymmetric separation and an upward deflected wake, as shown in Fig. 3.

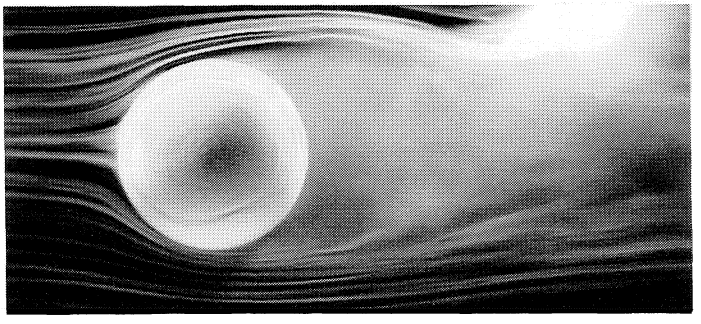

Figure 3: Flow visualization of a spinning tennis ball (flow is from left to right and the ball is spinning in a counter-clockwise direction).

Following Newton's 3rd Law of Motion, the upward deflected wake implies a downward (Magnus) force acting on the ball. Now the dependence of the boundary layer transition and separation locations on Re can either enhance or oppose (even overwhelm) this effect. Since the effective Re on the advancing side of the ball is higher than that on the retreating side, in the subcritical or (especially) supercritical regimes, the separation location on the advancing side will tend to be more upstream compared to that on the retreating side. This is because the C_D increases with Re in these regions, thus indicating an upstream moving separation location.

However, in the region of the critical Re, a situation can develop whereby the advancing side winds up in the supercritical regime with turbulent boundary layer separation, whereas the retreating side is still in the subcritical regime with laminar separation. This would result in a *negative* Magnus force, since the turbulent boundary layer on the advancing side will now separate later compared to the laminar layer on the retreating side. Therefore, a sphere with topspin for example, would experience an *upward* aerodynamic force. So in order to maximize the amount of (positive) Magnus force, it helps to be in the supercritical regime and this can be ensured by lowering the critical Re by adding surface roughness (e.g. dimples on a golf ball).

Baseball Aerodynamics

Baseball aficionados were not convinced that a baseball could actually curve until the late 1940s when some visual evidence was obtained and published. Two basic aerodynamic principles are used to make a baseball curve in flight: spin about an axis perpendicular to the line of flight and asymmetric boundary-layer separation due to seam location on non-spinning baseballs.

Let us first consider a pitch, such as the curveball, where spin is imparted to the baseball in an attempt to alter its flight just enough to fool the batter. The baseball for this particular pitch is released such that it acquires topspin about the horizontal axis. As discussed above, under the right conditions, this results in a (downward) Magnus force that makes the ball curve faster towards the ground than it would under the action of gravity alone. In Fig. 4, the flow over a spinning baseball is shown in a water channel using luminescent dyes at a relatively low Re (3400) and a spin rate parameter (S) of 2.5. The spin parameter is defined as the ratio of the equatorial velocity at the edge of the ball (V) to its translation velocity (U), hence S = V/U. At such a low Re, the flow over the baseball is expected to be subcritical, but the asymmetric separation and deflected wake flow are clearly evident, thus implying an upward Magnus force. Note the indentation in the dye filament over the upper surface due to the seam. At higher Re, the rotating seam would produce an effective roughness capable of causing transition of the laminar boundary layer. Spin rates of up to 35 revs/sec and speeds of up to 45 m/s (100 mph) are achieved by pitchers in baseball. Alaways (3) recently analyzed high-speed video data of pitched baseballs (by humans and a machine) and used a parameter estimation technique to determine the lift and drag forces on spinning baseballs. For a nominal pitching velocity range of 17 to 35 m/s (38 to 78 mph) and spin rates of 15 to 70 revs/sec, Alaways (3) gave a C_D range of 0.3 to 0.4. This suggests that the flow over a spinning baseball in this parameter range is in the supercritical regime with turbulent boundary layer separation. As discussed above, an asymmetric separation and a positive Magnus force would therefore be obtained in this operating range.

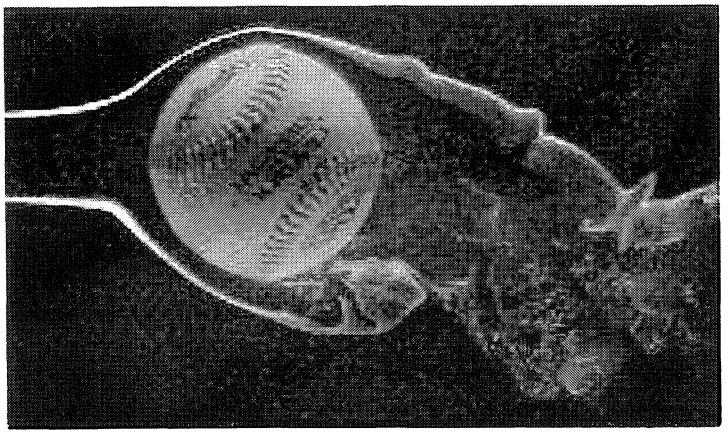

Figure 4: Flow visualization of a spinning baseball at Re = 3400 (flow is from left to right and the ball is spinning in a clockwise direction at 0.5 revs/sec). Photograph by Jim Pallis.

In some wind tunnel measurements of the lateral or lift force (L) on spinning baseballs, Watts and Ferrer (4) concluded that the lift force coefficient, C_L [= $L/(0.5\rho U^2 A)$] was a function of the spin parameter only, for S = 0.5 to 1.5, and at most only a weak function of Re, for Re = 30,000 to 80,000. Their trends agreed well with Bearman and Harvey's (5) golf ball data obtained at higher Re (up to 240,000) and lower spin parameter range (S = 0 to 0.3). Based on these correlations, Watts and Bahill (6) suggested that for spin rates typically encountered in baseball (S < 0.4), a straight line relation between C_L and S with a slope of unity is a good approximation. Alaways' lift measurements on spinning baseballs obtained for Re = 100,000 to 180,000 and S = 0.1 to 0.5, were in general agreement with the extrapolated trends of the data due to Watts and Ferrer. However, one main difference was that Alaways found a dependence of seam orientation (2-seam versus 4-seam) on the measured lift coefficient. The C_L was higher for the 4-seam case compared to the 2-seam for a given value of S. Watts and Ferrer (4) had also looked for seam orientation effects, but did not find any. Alaways concluded that the seam orientation effects were only significant for S < 0.5, and that at higher values of S, the data for the two orientations would collapse, as found by Watts and Ferrer (4). The main difference between these seam orientations is the effective roughness that the flow sees for a given rotation rate. As discussed above, added effective roughness puts the ball deeper into the supercritical regime, thus helping to generate the Magnus force. It is possible that at the higher spin rates (higher values of S), the difference in apparent roughness between the two seam orientations becomes less important.

The main significance of the seam orientation is realized when pitching the fastball. Fastball pitchers wrap their fingers around the ball and release it with backspin so that there is an upward (lift) force on the ball opposing gravity. The fastball would thus drop slower than a ball without spin and since there is a difference between the 2-seam and 4-seam C_L, the 4-seam pitch will drop even slower. However, even the 4-seam fastball cannot generate enough lift to overcome the weight of the ball, which is what would be needed to create the so-called "rising fastball." The maximum measured lift in Alaways' (3) study was equivalent to 48% of the ball's weight, so a truly rising fastball is not likely to occur in practice. A popular variation of the fastball is the split-finger and forkball. The split-finger, as the name implies, is held between the two pitching fingers and it is released with the same arm action and velocity as a regular fastball. Although some backspin is imparted to the ball, it is less than that for the fastball and it therefore drops a bit faster, thus giving it that sinker look. Apparently, and contrary to popular belief, the forkball is not quite the same pitch (Private Communication, LeRoy Alaways, 2000). For the forkball, the pitching fingers fork out and the ball is kept close to the palm with the thumb tucked under. The thumb is used to push the ball out and topspin is imparted to it, which produces an additional downward force and a flight trajectory below that of a ball with no spin.

The so-called "knuckleball" which is released with zero or very little spin has some very interesting aerodynamic characteristics. Watts and Sawyer (7) investigated the nature of the flow field by mounting a stationary baseball in a wind tunnel and measuring the lateral force for different seam orientations. Large values of the lateral force (up to ± 30% of the ball's weight) were measured with large fluctuations for the orientation when the seam coincided with the boundary-layer separation location. This was attributed to the separation location jumping between the front and back of the stitches, thus generating an unsteady flow field. Some very interesting flight paths were calculated for pitches where the ball was released with limited rotation (0.25 or 0.5 revolutions over 60.5 feet). Those experiments were performed at U = 21 m/s, which corresponds to Re of about 100,000. In Fig. 2, the baseball data are for a non-spinning baseball held in a symmetric orientation (the seams seen in Fig. 4 were in the horizontal plane and facing the flow). The critical Re is about 155,000 (U = 30 m/s) and so the flow regime in Watts and Sawyer's experiments was probably subcritical with laminar boundary layer separation. However, the present data suggest that if the ball was released at about 30 m/s (67 mph), then there exists a possibility of generating a turbulent boundary layer over parts of the

ball and hence a strong separation asymmetry and side force. Of course, note that the C_D versus Re trends and details of the generated flow fields will depend strongly on the seam orientation.

Golf Ball Aerodynamics

Golfing legend has it that in about the mid-nineteenth century, a professor in Scotland discovered that a gutta-percha ball flew farther when its surface was scored. This was the beginning of a ball design revolution in golf and it eventually led to dimples, which are an integral part of a golf ball cover design even today. In golf ball aerodynamics, apart from the lift force (which is generated by the backspin imparted to the ball), the drag and gravitational forces are also important, since the main objective is to "tailor" the flight path of the ball. The lift force is generated due to the Magnus effect and an example of the subcritical flow field over a spinning golf ball is given in Fig. 5. The asymmetric separation and downward deflected wake are both apparent and result in an upward lift force on the spinning golf ball. The effect of the dimples is to lower the critical Re, as shown in Fig. 2. Also, once transition has occurred, the C_D for the golf ball does not increase sharply in the supercritical regime, like that for the baseball, for example. This demonstrates that while the dimples are very effective at tripping the laminar boundary layer, they do not cause the thickening of the turbulent boundary layer associated with positive roughness.

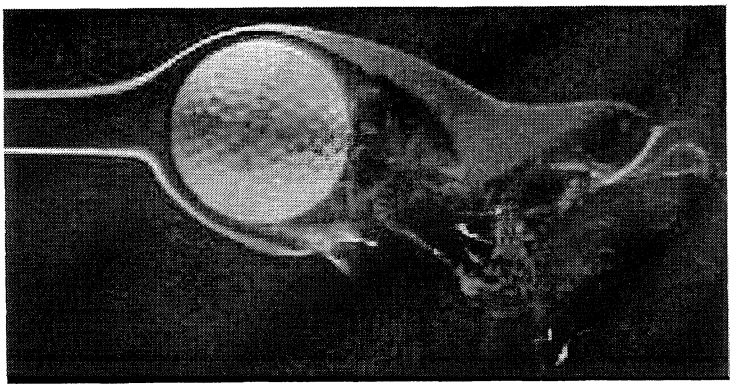

Figure 5: Flow visualization of a spinning golf ball at Re = 1950 (flow is from left to right and the ball is spinning in a clockwise direction at 0.5 revs/sec).

Bearman and Harvey (5) conducted a comprehensive study of golf ball aerodynamics using a large spinning model mounted in a wind tunnel over a wide range of Re (40,000 to 240,000) and S (0.02 to 0.3). They found that C_L increased monotonically with S (from about 0.08 to 0.25), as one would expect, and that the C_D also started to increase for $S > 0.1$ (from about 0.27 to 0.32) due to induced drag effects. The trends were found to be independent of Reynolds number for $126{,}000 < Re < 238{,}000$. More recently, Smits and Smith (8) made some wind tunnel measurements on spinning golf balls over the range, $40{,}000 < Re < 250{,}000$ and $0.04 < S < 1.4$, covering the range of conditions experienced by the ball when using the full set of clubs. Based on their detailed measurements, which included measurements of the spin decay rate, they proposed a new aerodynamic model of a golf ball in flight. Their measurements were in broad agreement with the observations of Bearman and Harvey, although the new C_L measurements were slightly higher (~ 0.04) and a stronger dependence of C_D on the spin parameter was exhibited over the entire S range. A new observation was that for $Re > 200{,}000$, a second decrease in C_D was observed, the first being that due to transition of the boundary layer. Smits and Smith proposed that this could be due to compressibility effects since the local Mach number over the ball reached values of up to 0.5. Note that Bearman and Harvey (5) used a 2.5 times larger model and so their Mach number was correspondingly lower. Smits and Smith (8) proposed the following model for driver shots in the operating range, $70{,}000 < Re < 210{,}000$ and $0.08 < S < 0.2$:

$C_D = C_{D1} + C_{D2}S + C_{D3} \sin\{\pi(Re - A_1)/A_2\}$

$C_L = C_{L1}S^{0.4}$

Spin Rate Decay = $\partial\omega/\partial t\ [d^2/(4U^2)] = R_1 S$

Suggested values for the constants are: $C_{D1} = 0.24$, $C_{D2} = 0.18$, $C_{D3} = 0.06$, $C_{L1} = 0.54$, $R_1 = 0.00002$, $A_1 = 90{,}000$ and $A_2 = 200{,}000$.

Over the years, several dimple designs and layouts have been tried to improve the golf ball aerodynamics. Bearman and Harvey (5) found that hexagonal dimples, instead of the conventional round ones, improved the performance of the ball since the C_L was slightly higher and the C_D lower. It was concluded that the hexagonal dimples were perhaps more efficient boundary layer trips by shedding discrete horse-shoe vortices from their straight edges. In order to try and minimize the amount of sideways deflection on an inadvertently sliced drive, a ball was designed (marketed under the name: "Polara") with regular dimples along a "seam" around the ball and shallower dimples on the sides. The ball is placed on the tee with the seam pointing down the fairway, and if only backspin about the horizontal axis is imparted to it, it will generate roughly the same amount of lift as a conventional ball. However, if the ball is heavily sliced, so that it rotates about a near-vertical axis, the reduced overall roughness increases the critical Re, and hence the sideways (undesirable) deflection is reduced. In an extreme version of this design, where the sides are completely bald, a reverse Magnus effect can occur towards the end of the flight which makes a sliced shot end up to the *left* of the fairway.

Tennis Ball Aerodynamics

Most of the recent research work on tennis ball aerodynamics was inspired by the introduction of a slightly larger "oversized" tennis ball (roughly 6.5% larger diameter). This decision was instigated by a concern that the serving speed in (men's) tennis had increased to the point where the serve dominates the game. The main evidence for the domination of the serve in men's tennis has been the increase in the number of sets decided by tie breaks at the major tournaments (9).

Some recent experimental studies of tennis ball aerodynamics have revealed the very important role that the felt cover plays (9-11). Fig. 6 shows a photograph of the smoke flow visualization over a 28-cm diameter tennis ball model that is held stationary (not spinning) in a wind tunnel. The first observation is that the boundary layer over the top and bottom of the ball separates relatively early, at $\theta_s \approx 80°$ to 90°, thus suggesting a laminar boundary layer separation. However, since the flow field did not change with Re (up to Re = 284,000), it was presumed that transition had already occurred and that a (fixed) turbulent boundary layer separation was obtained over the whole Re range tested, thus putting the ball in the transcritical flow regime. Although the felt cover was expected to affect the critical Re at which transition occurs, it seemed as though the felt was a more effective boundary layer trip than had been anticipated. The fact that the boundary layer separation over the top and bottom of the non-spinning ball was symmetric leading to a horizontal wake was, of course, anticipated since a side force (upward or downward) is not expected in this case.

In the second round of testing, spin was imparted to the ball by rotating the support rod. In Fig. 3, the ball is spun in a counter-clockwise direction to simulate a ball with topspin. The wind tunnel conditions corresponded to a standard tennis ball velocity of 39 m/s (87 mph) and spin rate of 72 revs/sec (4320 rpm); this would represent a typical second serve in men's professional tennis. In Fig. 3, the boundary layer separates earlier over the top of the ball compared to the bottom. As

discussed above, this results in an upward deflection of the wake behind the ball and a downward (Magnus) force acting on it which would make it drop faster than a non-spinning ball. By imparting spin to the ball, tennis players use this effect to make the ball curve; the direction and amount of movement is determined by the spin axis and the spin parameter (S). Spin about a near-vertical axis is imparted to gain sideways movement whereas topspin and underspin (or backspin) are used to control the trajectory length (shorter for topspin, longer for underspin).

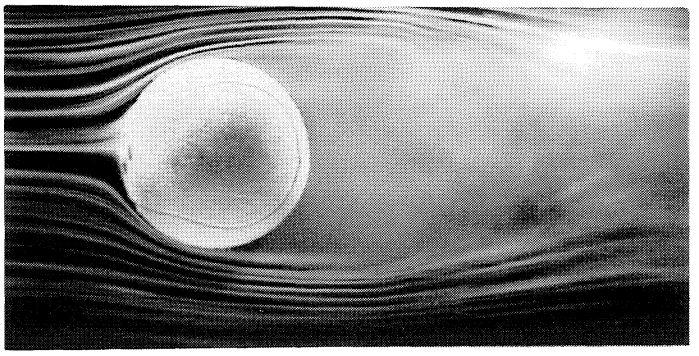

Figure 6: Flow visualization of a non-spinning tennis ball (flow is from left to right, Re = 167,000).

Drag measurements on non-spinning tennis balls (simulating a perfectly flat serve) revealed that, for the most part, the flow over new tennis balls was indeed transcritical, with a relatively high value for the drag coefficient ($C_D \cong 0.6$), higher than any other sports ball data shown in Fig. 2. In the transcritical regime, the turbulent boundary layer separation location has moved all the way up to the region of the ball apex, as shown in Fig. 6. Since almost all of the total drag on a bluff body, such as a round ball, is accounted for by pressure drag, it was proposed that the maximum C_D on a very rough sphere should not exceed 0.5 (11). However, on a tennis ball, apart from providing a rough surface, the felt cover is also a porous (drag-bearing) coating since the "fuzz" elements themselves experience pressure drag. This additional contribution was thus termed: "fuzz drag." Since the fuzz elements come off as the ball surface becomes worn, the ball C_D should also decrease, and that is precisely what was observed in the data for the used ball (Fig. 2). The used ball appears to be in the supercritical regime with a critical Re $\approx$ 100,000.

One of the more intriguing trends in the (new) tennis ball drag measurements was the increase in C_D with decreasing Re. The higher levels of C_D at the lower Re ($80{,}000 < Re < 150{,}000$) were attributed to the dependence of fuzz element orientation on flow (or ball) velocity and the stronger dependence of C_D on Re at the very low fuzz element Re. The recently approved oversized tennis ball C_D was found to be comparable to that for the standard-sized balls. However, the drag on the oversized balls is higher by virtue of the larger cross-sectional area and so the desired effect of "slowing down the game" (increased ball flight time) will be achieved.

Cricket Ball Aerodynamics

Aficionados know cricket as a game of infinite subtlety, not only in strategy and tactics, but also in its most basic mechanics. On each delivery, the ball can have a different trajectory, varied by changing the pace (speed), length, line or, most subtly of all, by moving or "swinging" the ball through the air so that it drifts sideways. The actual construction of a cricket ball and the principle by which the faster bowlers swing the ball is unique to cricket. A cricket ball has six rows of prominent stitching along its equator, which makes up the "primary" seam. Each hemisphere also has a line of internal stitching forming the "quarter" or "secondary" seam. These primary and quarter seams play a critical role in the aerodynamics of a swinging cricket ball (12).

Fast bowlers in cricket make the ball swing by a judicious use of the primary seam. The ball is released with the seam at an angle to the initial line of flight. Over a certain Reynolds number range, the seam trips the laminar boundary layer into turbulence on one side of the ball whereas that on the other (nonseam) side remains laminar. As discussed above, by virtue of its increased energy, the turbulent boundary layer, separates later compared to the laminar layer and so a pressure differential, which results in a side force, is generated on the ball. In Fig. 7, the seam has tripped the boundary layer on the lower surface into turbulence, evidenced by the chaotic nature of the smoke edge just downstream of the separation point. On the upper surface, a smooth, clean edge confirms that the separating boundary layer is in a laminar state. Note how the laminar boundary layer on the upper surface has separated relatively early compared to the turbulent layer on the lower surface. The asymmetric separation of the boundary layers is further confirmed by the upward deflected wake, which implies that a downward force is acting on the ball.

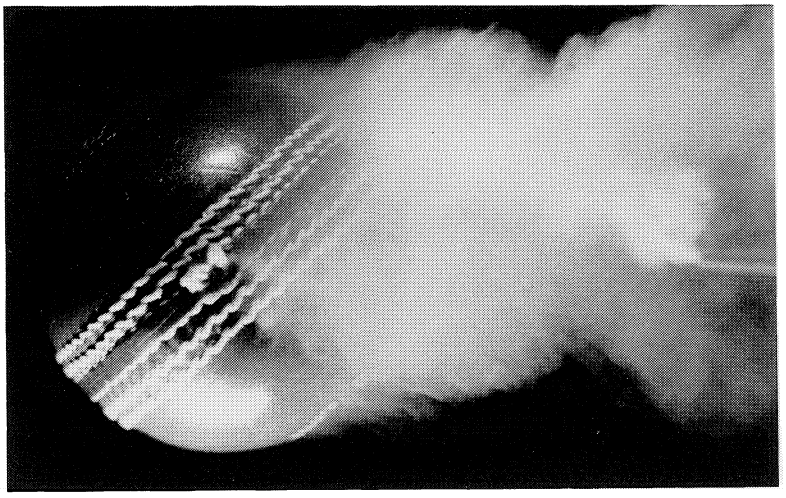

Figure 7: Flow visualization over a cricket ball (flow is from left to right, seam angle = 40°, U = 17 m/s, Re = 85,000).

When a cricket ball is bowled, with a round arm action as the laws insist, there will always be some backspin imparted to it as the ball rolls-off the fingers as it is released. In order to measure the forces on spinning cricket balls, cricket balls were rolled along their seam down a ramp and projected into a wind tunnel through a small opening in the ceiling (12). The aerodynamic forces were evaluated from the measured deflections. At nominally zero seam angle there was no significant side force, except at high velocities when local roughness, such as an embossment mark, starts to have an effect by inducing transition on one side of the ball. However, when the seam was set at an incidence to the oncoming flow, the side force started to increase at about U = 15 m/s (34 mph). The side force increased with ball velocity, reaching a maximum of about 30% of the ball's weight before falling-off rapidly. The critical velocity at which the side force started to decrease was about 30 m/s (Re = 140,000). This is the velocity at which the laminar boundary layer on the nonseam side undergoes transition and becomes turbulent. As a result, the asymmetry between the boundary layer separation locations is reduced and the side force starts to decrease. The C_D curve for the cricket ball in Fig. 2 seems to indicate that transition has started to occur at Re < 140,000. For those tests, the (non-spinning) ball was released with the seam angled at 20° and it was found that the ball rotated due to the aerodynamic moment about the vertical axis and thus the seam caused relatively early transition on both sides of the ball. Also, these data suggest that as the critical Re is approached, the C_D for spinning balls will not fall-off as abruptly as that for non-spinning balls. On spinning balls, the transition occurs in stages led by the advancing side where the effective Re is higher. Also, note that for balls with discrete roughness (seam on cricket ball and baseball), the spin axis and rotation rate also play an important role in determining the ball aerodynamics.

The maximum side force was obtained at a bowling speed of about 30 m/s (67 mph) with the seam angled at 20° and the ball spinning backwards at a rate of 11.4 revs/s. Trajectories of a cricket ball, computed using the measured forces, resulted in a parabolic flight path with a maximum deflection of 0.8 m; this compared extremely well with field measurements. The computed data also helped to explain the phenomenon of "late" swing. Since the flight paths are parabolic, late swing is in fact "built-in" whereby 75% of the lateral deflection occurs over the second half of the flight from the bowler to the batsman. A used ball with a rough surface can be made to "reverse swing" at relatively high bowling speeds. Due to the rough surface, transition occurs relatively early (before the seam location) and symmetrically. The seam acts as a fence, thickening and weakening the turbulent boundary layer on that (seam) side which separates early compared to the turbulent boundary layer on the nonseam side. Therefore, the whole asymmetry is reversed and the ball swings *towards* the nonseam side.

Volleyball and Soccer Ball Aerodynamics

In recent years, there has been an increased interest in the aerodynamics of volleyballs and soccer balls. In volleyball, two main types of serves are employed: a relatively fast spinning serve (generally with topspin), which results in a downward Magnus force adding to the gravitational force or the so-called "floater" which is served at a slower pace, but with the palm of the hand so that no spin is imparted to it. An example of a serve with topspin is shown in Fig. 8. The measured flight path implies that the downward force (gravity plus Magnus) probably does not change significantly, thus resulting in a near-parabolic flight path. The floater has an unpredictable flight path, which makes it harder for the returning team to set up effectively.

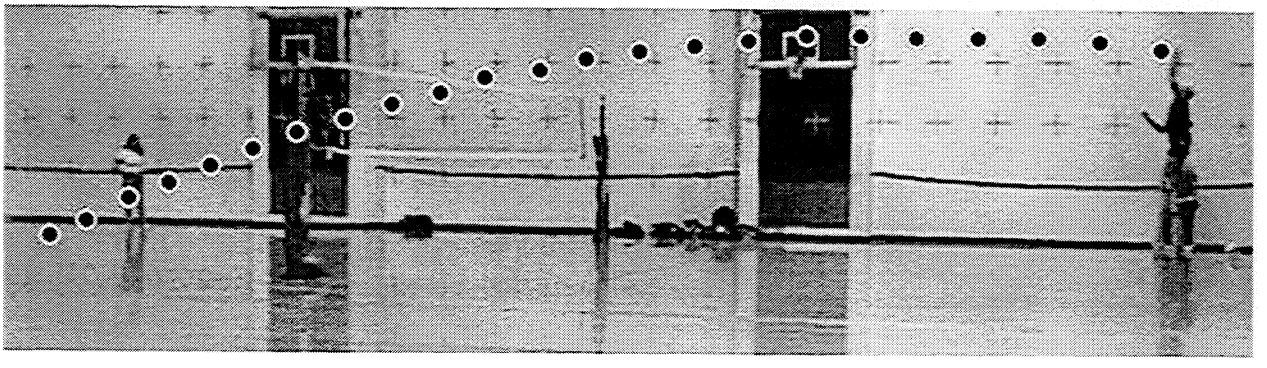

Figure 8: Measured trajectory of a volleyball serve with topspin (courtesy of Tom Cairns, Mathematics Department, The University of Tulsa).

In soccer, the ball is almost always kicked with spin imparted to it, generally backspin or spin about a near-vertical axis, which makes the ball curve sideways. The latter effect is often employed during free kicks from around the penalty box. The defending team puts up a "human wall" to try and protect a part of the goal, the rest being covered by the goalkeeper. However, the goalkeeper is often left helpless if the ball can be curved around the wall. A recent spectacular example of this type of kick was in a game between Brazil and France in 1997 (13). The ball initially appeared to be heading far right of the goal, but soon started to curve due to the Magnus effect and wound up "in the back of the net." A "toe-kick" is also sometimes used in the free kick situations to try and get the "knuckling" effect.

For both these balls, the surface is relatively smooth with small indentations where the "patches" come together, so the critical Re would be expected to be less than that for a smooth sphere, but higher than that for a golf ball. As seen in Fig. 2, that is indeed the case for a non-spinning volleyball with a critical Re of about 200,000. The typical serving speeds in volleyball range from about 10 m/s to 30 m/s and at Re = 200,000, U = 14.5 m/s. So it is quite possible to serve at

a speed just above the critical (with turbulent boundary layer separation) and as the ball slows through the critical range, get side forces generated as non-uniform transition starts to occur depending on the locations of the patch-seams. Thus, a serve that starts off on a straight flight path (in the vertical plane), may suddenly develop a sideways motion towards the end of the flight. Even in the supercritical regime, wind tunnel measurements have shown that side force fluctuations of the same order of magnitude as the mean drag can be developed on non-spinning volleyballs, which can cause the "knuckling" effect (14).

REFERENCES

1. R.D. Mehta, "Aerodynamics of Sports Balls," Annual Review of Fluid Mechanics, 17 (1985), 151-189.

2. E. Achenbach, "Experiments on the Flow Past Spheres at Very High Reynolds Number," Journal of Fluid Mechanics, 54 (1972), 565-575.

3. L.W. Alaways, "Aerodynamics of the Curve-Ball: An Investigation of the Effects of Angular Velocity on Baseball Trajectories" (Ph.D. dissertation, University of California, Davis, 1998).

4. R.G. Watts and R. Ferrer, "The Lateral Force on a Spinning Sphere: Aerodynamics of a Curveball," American Journal of Physics, 55 (1987), 40-44.

5. P.W. Bearman and J.K. Harvey, "Golf Ball Aerodynamics," Aeronautical Quarterly, 27 (1976), 112-122.

6. R.G. Watts and A.T. Bahill, Keep your eye on the ball: Curve balls, Knuckleballs, and Fallacies of Baseball (New York, NY: W. H. Freeman, 2000).

7. R.G. Watts and E. Sawyer, "Aerodynamics of a Knuckleball," American Journal of Physics, 43 (1975), 960-963.

8. A.J. Smits, A.J. D.R. Smith, "A New Aerodynamic Model of a Golf Ball in Flight," Science and Golf II, ed. A.J. Cochran (London, UK: E. & F.N. Spon, 1994), 341-347.

9. S.J. Haake, S.G. Chadwick, R.J. Dignall, S. Goodwill, and P. Rose, P. "Engineering Tennis - Slowing the Game Down," Sports Engineering, 3 (2) (2000), 131-143.

10. A.J. Cooke, "An Overview of Tennis Ball Aerodynamics," Sports Engineering, 3 (2) (2000), 123 - 129.

11. R.D. Mehta and J.M. Pallis, "The Aerodynamics of a Tennis Ball," submitted to Sports Engineering, January 2001.

12. R.D. Mehta, "Cricket Ball Aerodynamics: Myth Versus Science," The Engineering of Sport. Research, Development and Innovation, ed. A.J. Subic and S.J. Haake (Oxford, UK: Blackwell Science, 2000), pp. 153 – 167.

13. T. Asai, T. Akatsuka, and S. Haake "The Physics of Football," Physics World, 11-6 (1998), 25-27.

14. Q. Wei, R. Lin, and Z. Liu, "Vortex-Induced Dynamic Loads on a Non-Spinning Volleyball," Fluid Dynamics Research, 3 (1988), 231-237.